Inverse Energy-Uncertainty Relation for a Simple Information Engine

Bradley Chase* and Alfred Hübler†
Santa Fe Institute, 1399 Hyde Park Road, Santa Fe, NM 87501
(Dated: August 15, 2005)

We examine the relationship between uncertainty in initial conditions and subsequent energy gain for a simple information engine in the likeness of Maxwell's Demon. Our engine consists of two noninteracting idealized classical particles in a two-compartment box. Using information about the initial states of the particles and our uncertainty in those states, we desire to capture both particles to perform work. We find that in certain cases the energy extracted is inversely proportional to the initial uncertainty. We also examine properties of a nonlinear container. We also note that the average energy over all initial condition cases is approximately the fraction of particles which we can predict long enough for the possibility of capture to occur.

PACS numbers: 05.10.-a,05.20.-y,05.70.-a

An inchoate relationship between information and energy was borne from attempts to resolve the paradoxical violation of the second law of thermodynamics introduced by Maxwell's Demon [1]. Work by Szilard, which thrust the concept of information into the analysis, coupled with later work by Bennet regarding entropy and irreversible computation, accounted for the needed increase in entropy in terms of the necessary erasure of the demon's memory about the system [2, 3]. This link between information and entropy serves as a foundation for the creation of a machine which utilizes information to perform work. Recent investigations into such an information-engine focus on the thermodynamics of fluctuation-induced transport and depend upon nonequilibrium fluctuations to perform work [4–6]. Other work by Bekenstein derived a relationship between energy and gravitational entropy by studying black holes [7]. Lloyd investigated quirks introduced by considering a quantum incarnation of Maxwell's Demon as well as the feasibility of an information engine in terms of a system's ability to obtain information about another system [8, 9]. More genereally, other work has focused on the use of information for efficiency purposes, such as air condition control and even tax control on the use of fossil fuel energy sources [10].

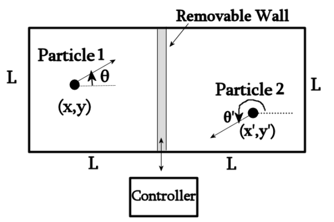

FIG. 1: Information-Uncertainty engine inspired by Maxwell's Demon

Rather than concentrate on the thermodynamic relationship between entropy and energy, we focus instead on the relationship between initial uncertainty and work done in a particular system. As depicted in Fig. 1, our information engine consits of two noninteracting particles, moving at constant velocity within two equal sized compartments of a two-dimensional box. Each particle is parametrized by a position and direction. Assuming constant velocity, the each particle's motion is described by

$$\vec{x}_1 = \vec{x}_0 + t\vec{v} \tag{1}$$

The particles reflect off walls elastically according to

$$\vec{v}_{\text{new}} = \vec{v}_{\text{old}} - (2\vec{v}_{\text{old}} \cdot \vec{N})\vec{N} \tag{2}$$

where $\vec{N}$ is the unit surface normal of the wall. A partition wall can be inserted or removed with arbitrary speed in order to trap the particles in compartments. Simplifying our goal of capturing both particles in the same compartment, we designate the right compartment of the box as the target. Each particle has some associated uncertainty $\delta\theta_0$ in the initial direction and machine precision initial uncertainty in position, δx_0 or δy_0, or velocity, δv_0. The directions of the ensemble particles are then drawn from the probability distribution

$$P(\theta) = \begin{cases} \frac{1}{2\delta\theta_0} \text{ for } \theta_0 - \delta\theta_0 < \theta < \theta_0 + \delta\theta_0 \\ 0 \text{ otherwise} \end{cases} \tag{3}$$

This can be considered band-limited white noise, where the bandwith is specified by $B = 2\delta\theta_0$. Another way to interpret the uncertainty in direction is as the information entropy of the direction, which would be $S = \ln(2\delta\theta_0)$ for the above. The initial entropy for the system is then $S_s = k \ln \Omega_0$ where k is the Boltzmann constant and $\Omega_0 = v_0\delta v_0\delta\theta_0\delta x_0\delta y_0 v_0'\delta v_0'\delta\theta_0'\delta x_0'\delta y_0'$ with the unprimed quantities denoting particle one and the primed quantities denoting particle two.

The wall is operated by an ensemble predictor, which uses the simulated behavior of an ensemble of particle trajectories to predict when the right particle might hit

---

*Also at Rice University; Electronic address: bchase@rice.edu
†Also at University of Illinois, Urbana-Champaign

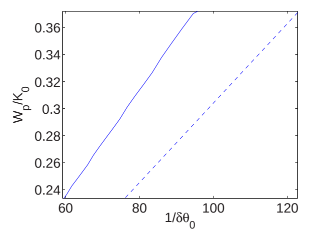

FIG. 2: Fraction of energy extracted versus the inverse of the uncertainty in initial direction for initial condition near the center of the box. Ensemble Simulation (dashed) and Theoretical Predictions (solid), Eq. (9)

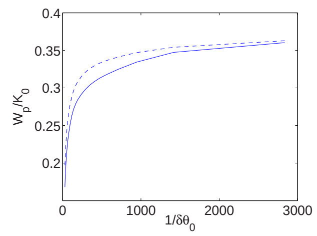

FIG. 3: Fraction of energy extracted versus uncertainty in initial direction for an ensemble of initial conditions

the partition wall. Such a controller would itself require energy to compute, as might the operation of the wall, but that is not considered here. The controller simulation proceeds using a small timestep evaluation of Eq. (1), checking for wall collisions and reflecting the simulated particles if necessary. This simulation gives some probability $P_l(t)$ and $P_r(t)$ of the left or right particle hitting the partition wall. The controller keeps the partition wall open unless the right particle might escape, which occurs if $P_r(t) = 1$ for the right particle.

Assuming an adiabatic expansion of an ideal gas with two degrees of freedom, we can extract $\frac{3}{8}K_0$ of the initial energy K_0 of the particles by capturing them together in the right partition. Given the initial conditions of each particle and the uncertainty in those quantities, there is a probability P_c of capturing both particles on the same side of the box. Hence the amount of energy that can be extracted in terms of the initial energy is$W_p = P_c\frac{3}{8}K_0$. Fig. 2, shows the results of a simulation which imply

$$\frac{W_p}{K_0} \propto \frac{1}{\delta\theta_0} \tag{4}$$

We observed numerically where each particle starts in the center of its container and $\theta_{0_{\text{left}}} = \frac{3.3\pi}{5}$ and $\theta_{0_{\text{right}}} = \frac{\pi}{3}$. The above simulation depicts one class of behavior, in which the particle partition wall hit times overlap. There are also cases where these hit times do not overlap and we instead see $P_c = 1$ or $P_c = 0$ over large ranges of initial uncertainty in direction. We examined the average case behavior by dividing each coordinate axis(x,y,θ) into N points, giving N^3 initial positions. As seen in Fig. 3, we found that only five percent of initial left particle and right particle conditions results in overlapping hit times, while the remaining pairs of initial conditions resulted in non overlapping hit times.

For an analytical model of the system, we approximate the dynamics of the particles in terms of a series of wall collisions. Each successive wall collision can be interpreted as a new system describing the particle with different initial conditions and uncertainties. Following the iterative simulation process of the controller, we can generate a time series indicating when either particle hits the partition wall and the associated uncertainty in that time. There will be some time, t_s, after which the controller keeps the wall closed. Using the time series, we can calculate the probability of capturing the particles together in the following manner. Let $P_r(t)$ represent when the particle in the target container hits the removable wall and $P_l(t)$ represent when the particle in the other container hits the removable wall. Since we keep the wall open unless the particle in the right container hits the partition, the probability of catching the particle, P_c as

$$P_c = \int_0^{t_s} (1 - \Theta(P_r(t)))P_l(t)dt \tag{5}$$

where $\Theta(t)$ is 1 if its argument is non-zero and is 0 otherwise.

In order to generate the aforementioned time series $P_r(t)$ and $P_l(t)$, we need to be able to predict which wall a given particle will hit. By drawing unit vectors to each corner of the box from the current particle position, we are able to partition the box into four regions corresponding to the four walls. Based on which partition the current direction falls within, we can determine which wall is hit. However, there is some uncertainty in the current direction as well as the unit vectors to the corners, so if the controller is unable to uniquely pick a partition for the current direction, the partition wall remains closed from time t_s on.

Detailed calculations for propagated uncertainty and the wall-angle determination are available in [11]. However, we generally note for some quantity q_j, the associated uncertainty on the i-th bounce is given by

$$\delta q_{j_i} = \sum_k \delta q_{k_{i-1}} \left| \frac{\partial q_j(q_{1_{i-1}}, q_{2_{i-1}}, \ldots)}{\partial q_k} \right| \tag{6}$$

Iterating this equation, we have

$$\delta q_{j_i} = \sum_{k_i} \sum_{k_{i-1}} \cdots \sum_{k_1} \delta q_{k_0} \left| \frac{\partial q_j(q_{1_0}, \ldots)}{\partial q_{k_0}} \right| \cdots \left| \frac{\partial q_j(q_{1_{i-2}}, \ldots)}{\partial q_{k_{i-1}}} \right| \left| \frac{\partial q_j(q_{1_{i-1}}, \ldots)}{\partial q_{k_i}} \right| \tag{7}$$

where the partial derivatives are determined by the geometry of the box. We see that when varying only the initial uncertainty while fixing the geometry and initial conditions, the propagated uncertainty depends linearly on the initial uncertainty. This linear relation is independent of the particular container geometry.

Trivially, Eq. (5) implies P_c is 0 or 1 if the partition wall hit times of the particles do not overlap. Nontrivially, there are 3 cases of overlap. Consider $P_r(t)$ and $P_l(t)$ as uniform distributions centered about hit times t_{r_i} and t_{l_i} with widths $2\delta t_{r_i}$ and $2\delta t_{l_i}$ for bounce i. If $t_{r_i} < t_{l_i}$ and $t_{l_i} - t_{r_i} \leq \delta t_{r_i} + \delta t_{l_i}$ (case 1),

$$P_c = \frac{(t_{l_i} + \delta t_{l_i}) - (t_{r_i} + \delta t_{r_i})}{2\delta t_{l_i}} = \frac{(t_{l_i} - t_{r_i}) - \delta t_{r_i}}{2\delta t_{l_i}} + \frac{1}{2}$$

If $t_{r_i} > t_{l_i}$ and $t_{r_i} - t_{l_i} \leq \delta t_{r_i} + \delta t_{l_i}$ (case 2),

$$P_c = \frac{(t_{r_i} - \delta t_{r_i}) - (t_{l_i} - \delta t_{l_i})}{2\delta t_{l_i}} = \frac{(t_{r_i} - t_{l_i}) - (\delta t_{r_i})}{2\delta t_{l_i}} + \frac{1}{2}$$

If $\delta t_{r_i} < \delta t_{l_i}$,$t1 + \delta t_{r_i} < t_{l_i} + \delta t_{l_i}$ and $t_{r_i} - \delta t_{r_i} > t_{l_i} - \delta t_{l_i}$ (case 3)

$$P_c = \frac{2\delta t_{l_i} - 2\delta t_{r_i}}{2\delta t_{l_i}} = -\frac{\delta t_{r_i}}{\delta t_{l_i}} + 1$$

Suppose we have a situation with $a, b,$ and c overlaps of cases 1, 2 and 3 respectively, where $a + b + c = n$. The overall capture probability is then

$$\begin{aligned} P_c &= \frac{1}{n}\left[\sum_{i=1}^{a+b}\left(\frac{1}{2} + \frac{C_i - \delta t_{r_i}}{2\delta t_{l_i}}\right) + \sum_{i=1}^{c}\left(1 - \frac{\delta t_{r_i}}{\delta t_{l_i}}\right)\right] \\ &= \frac{1}{n}\left[\frac{a}{2} + \frac{b}{2} + c + \sum_{i=1}^{a+b}\frac{C_i - \delta t_{r_i}}{2\delta t_{l_i}} - \sum_{i=1}^{c}\frac{\delta t_{r_i}}{\delta t_{l_i}}\right] \\ &= \frac{1}{2} + \frac{c}{2n} + \frac{1}{n}\left[\sum_{i=1}^{a+b}\frac{C_i - \delta t_{r_i}}{2\delta t_{l_i}} - \sum_{i=1}^{c}\frac{\delta t_{r_i}}{\delta t_{l_i}}\right] \end{aligned} \tag{8}$$

If we only vary $\delta\theta_0$ such that we can assume $\delta t_{r_i} \approx \delta t_{l_i}$, then $\delta t_{l_i} = d_i \delta\theta_0$ by Eq. (7), with d_i representing the product of the partial derivatives. Letting $C_i = t_{r_i} - t_{l_i}$, Eq. (8) simplifies to

$$P_c =< \frac{C_i}{2\delta t_{l_i}} >= \frac{M}{\delta\theta_0} \tag{9}$$

where $M =< \frac{C_i}{2d_i} >$. This equation gives the theoretical estimate of the inverse energy-uncertainty relation Eq. (4) as depicted in Fig. (2).

Verification of this relation was done via computer simulation. An ensemble of particles were simulated, distributed uniformly to represent the uncertainty in the initial We observed numericallydirection θ_0 and their trajectories were simulated using a small timestep. The fraction of initial particles released and captured gave the probability of capture. These results were compared with closed form estimates based off of equation Eq. (8).

We also examined the relation for a curved container, in which the top wall of the target container was curved. The radius of curvature, R, was also varied. In this case, the propagated uncertainty in direction is not constant, due to the nonlinear spreading of nearby trajectories. As seen in Fig. 4 we get the inverse energy-uncertainty relation as predicted by the analytical approach. However, in Fig. 5, we see that the greater the curvature, the lesser the constant of proportionality M between extracted energy and uncertainty. A linear least-squares fit of the curve for particles with initial conditions near the center of each partition gives

$$M = \frac{-31.73}{R} + 1.2691 \tag{10}$$

Since the curved wall results in a faster increase in propagated uncertainty, P_c does not increase as quickly as the linear case for a similar decrease in initial uncertainty.

In order to get a sense of the overall energy relationship, we averaged over all possible particle starting positions and directions, varying initial uncertainties. Computationally, this meant we divided each coordinate axis into N initial points, giving N^3 possible initial conditions per particle. For a given uncertainty, we tabulated the hit times and uncertainties according to the derived error equations. P_c was then calculated pairwise for all initial conditions. These N^6 probabilities were then averaged. The results can be seen in Fig. 3. From the simulation, we observed that about five percent of initial condition pairs resulted in overlapping hit times. The remaining pairs of particles are of the trivial case for which P_c is either 0 or 1. However, the ratio of those pairs which is 0 or 1 changes with uncertainty. The probability of capture P_c is then approximately the ratio of the number of successful captures ($P_c = 1$) to the number of initial condition pairs. Since the trivial case is governed by whether a particle impacts the partition wall before the stop time t_s, a good estimate is to consider the fraction of initial particles which become unpredictable prior to hitting the partition wall. If N_n represents the number of particles in the simulation which never hit the partition wall before

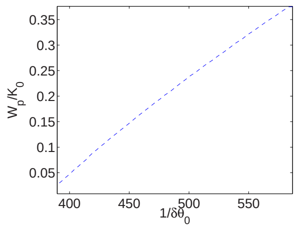

FIG. 4: Fraction of energy extracted versus the inverse of the uncertainty in initial direction, curved wall $R = 25$

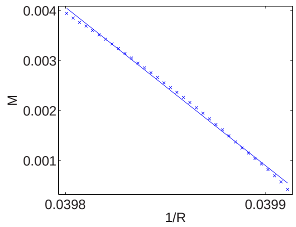

FIG. 5: Proportionality constant M versus curvature of container surface $1/R$. Simulation (crosses) and Linear Least-Squares Fit (solid line)

t_s, the estimate is

$$P_{\rm E} = \frac{(N^3 - N_n)^2}{N^6} \tag{11}$$

which implies that the first bounce is the most critical in determining capture. Since the unpredictability test depends acutely on the geometry of the compartments, we did not devise an analytic relation.

Additionally, we can compare our efficiency to the thermodynamical limits for the system. Given that $S = k \ln \Omega$, and $\Delta S = \frac{\Delta W}{T}$ for a reversible process, we find that $W = K_0 \left(1 - \frac{\Omega_0}{\Omega_f}\right)$. For our system, we assume the uncertainties for Ω_f are the size of the box for $\delta x_f, \delta y_f$, 2π for $\delta\theta_f$ and v_i for both v_f and δv_f. By this argument, we can essentially extract all of the initial energy K_0 from the system to perform work, which is much more efficient than the information engine presented in this paper.

We have demonstrated that work done or energy extracted is inversely proportional to initial uncertainty for our simple information engine. Additionally, we have shown that on average, the energy extracted can be estimated by the percentage of particles which have at least one chance to cross the barrier wall. We believe these conclusions provide insight into the nature of information engines and provide an excellent starting point for further study of the properties of such engines. Future considerations include examining quantum effects, varying the number of particles, the energy requirements of the controller, and alternative controller strategies which might make a more efficient conversion possible.

This research was done as part of an NSF sponsored REU program at the Santa Fe Institute and support by National Science Foundation Grants No. NSF PHY 01-40179, NSF DMS 03-25939 ITR, and NSF DGE 03-38215.

[1] J. C. Maxwell, *Theory of Heat* (Longmans, Green, And Co., London, 1871).
[2] L. Szilard, Z. f. Physik **53**, 840 (1929).
[3] C. H. Bennet, Sci. Am. **257** (1987).
[4] M. M. Millonas, Phys. Rev. Lett. **74** (1995).
[5] A. M. Jayannavar, Phys. Rev. E **53** (1996).
[6] C. R. Doering, W. Horsthemke, and J. Riordan, Phys. Rev. Lett. **72**, 2984 (1994).
[7] J. D. Bekenstein, Phys. Rev. D **23**, 287 (1981).
[8] S. Lloyd, Phys. Rev. A **56**, 3374 (1997).
[9] S. Lloyd, Phys. Rev. A **39**, 5378 (1989).
[10] A. M. Weinberg, Interdisciplinary Sci. Rev. **7**, 42 (1982).
[11] B. Chase and A. Hübler (2005), unpublished SFI REU Report.